

57-Year California Reanalysis Downscaling at 10 km (CaRD10)

-- Part 2. Comparison with North American Regional Reanalysis --

by

Hideki Kanamaru and Masao Kanamitsu

Scripps Institution of Oceanography

University of California, San Diego

for publication in *Journal of Climate*

Submitted May 7, 2006
Revised December 6, 2006
Second Revision March 7, 2007

Corresponding author: Dr. Hideki Kanamaru, Mail Code 0224; CRD/SIO/UCSD; 9500 Gilman Drive; La Jolla, CA 92093-0224
E-mail: hkanamaru@ucsd.edu

Abstract

The California Reanalysis Downscaling at 10 km (CaRD10) was compared with the North American Regional Reanalysis (NARR) which is a data assimilation regional analysis at 32 km resolution and 3hourly output using the Eta model for the period 1979-present using the NCEP/DOE Reanalysis as lateral boundary conditions. The objectives of this comparison are two fold; 1) to understand the efficacy of regional downscaling and horizontal resolution and 2) to estimate the uncertainties in regional analyses due to system differences.

The large-scale component of atmospheric analysis is similar in CaRD10 and NARR. The CaRD10 daily winds fit better to station observations than NARR over ocean where daily variability is large, and over land. The daily near-surface temperature comparison shows a similar temporal correlation with observations in CaRD10 and NARR. Several synoptic examples such as the Catalina Eddy, Coastally Trapped Wind Reversal, and Santa Ana winds are better produced in CaRD10 than NARR. These suggest that the horizontal resolution of the model has a large influence on the regional analysis, and the near-surface observation is not properly assimilated in the current state-of-the-art regional data assimilation system.

The CaRD10 near-surface temperature and winds on monthly and hourly scales are similar to NARR with more regional details available in CaRD10. The Southwestern monsoon is poorly reproduced in CaRD10 due to the position of the lateral boundary. The spatial pattern of the two precipitation analyses is similar but CaRD10 shows smaller scale features despite a positive bias. The trends of 500-hPa height and precipitation are similar in the two analyses but the near-surface temperature trend spatial patterns do not agree, suggesting the importance of regional topography, model physics, and land surface schemes. A comparison of a major storm event shows that both analyses suffer from budget residual. CaRD10's large precipitation is

related to wind direction, spatial distribution of precipitable water, and a large moisture convergence.

Dynamical downscaling forced by a global analysis is a computationally economical approach to regional scale long-term climate analysis and can provide a high quality climate analysis comparable to current state-of-the-art data assimilated regional reanalysis. However, uncertainties in regional analyses can be large and caution should be exercised when using them for climate applications.

Introduction

The detailed description of the CaRD10 (California Reanalysis Downscaling at 10 km) downscaling system and the verification of the product comparing to station observation were presented in the Part 1 of this two-part paper (hereafter referred to as Part 1; Kanamitsu and Kanamaru, 2006). In summary, it was shown that the downscaled analysis fits much better to regional scale station observations than the coarse resolution NCEP/NCAR Reanalysis used to force the regional model, supporting the premise that the regional downscaling is a viable method to attain regional detail from large-scale analysis without regional data assimilation.

Recently, high-resolution regional reanalysis over North America was conducted by NCEP (North American Regional Reanalysis (NARR), Mesinger et al, 2006). NARR is a comprehensive effort to produce historical high-resolution analysis over North America using a state-of-the-art variational data assimilation system utilizing various types of high spatial resolution satellite observation, surface observation and gridded observed precipitation. NARR was performed with the horizontal resolution of 32 km and three hourly outputs for the period of 1979 to present.

The CaRD10 project was designed to produce a long term, high resolution climate dataset over California. CaRD10 does not cover NARR's large area, nor does it use any of the regional scale observations NARR uses. However three unique features distinguish CaRD10 from NARR – 10 km horizontal resolution, hourly output and coverage of 1948 to present.

This paper has two primary objectives. The first is to understand the ability of regional downscaling and the state-of-the-art data assimilation system which uses near-surface observations, and the role of horizontal resolution in regional analyses. The second is to estimate the uncertainties in regional analyses. A comparison of these two analyses provides uncertainties

in the regional analyses which are difficult to assess without multiple independent regional analyses.

The comparison of CaRD10 and NARR is not exactly analogous to the comparison of two reanalyses because of the large differences in these two analysis systems. CaRD10 is a dynamically downscaled analysis of NCEP/NCAR Reanalysis (NNR; Kalnay et al. 1996). The dynamical downscaling technique with the scale selective bias correction scheme (Kanamaru and Kanamitsu 2007) used in CaRD10 is discussed in Part 1. NARR is a regional reanalysis with assimilation of observations using NCEP/DOE Reanalysis (Kanamitsu et al. 2002) as a lateral boundary condition. The forecast model used in CaRD10 is based on sigma-coordinate Regional Spectral Model (RSM) and its physical processes were taken from the NCEP seasonal forecast model. On the other hand, the model used in NARR is an eta-coordinate grid-point model with physical processes quite different from RSM.

There are several major differences between the observations used in NNR (large-scale forcing for CaRD10) and NARR. For example NNR uses satellite-retrieved temperature but NARR uses raw radiance observation and more surface observations. Major differences are expected in the regional scale, but not in the large-scale components (see section 2). It should be noted that NARR does not use 2-meter temperature observation over land. Also, although near-surface winds and humidity are used in NARR, their impact on the analysis was found to be “marginal” (Mesinger et al. 2006). Surface pressure is likely to be a small-scale observation that had more impact on NARR, but how much this observation affects the analysis of other variables is not very clear. Accordingly, the dense surface observations in NARR may not make a large contribution to its resulting analysis. In addition to surface observations, NARR uses observed

gridded precipitation in the data assimilation, which adds small-scale features in the precipitation observation and changes temperature profile and specific humidity.

First of all, it is essential to understand the difference in surface topography between CaRD10 and NARR, which is probably one of the greatest factors accounting for the difference in surface variables. Figure 1a,b shows the surface height in CaRD10 and NARR, respectively, and 1c shows the surface height difference between the two. The largest difference is in the Sierra Nevada Mountains where CaRD10 is higher than NARR by as much as 800 m on the windward side of the mountain range, and lower by up to 600 m on the lee side.

The paper is organized as follows. In section 2, the large-scale analyses between CaRD10 and NARR are compared. In section 3, the fit of the analyses to station observations is discussed. Section 4 presents comparisons of several synoptic scale events. These two sections (3 and 4) aim at examining the efficacy of regional downscaling and the importance of horizontal resolution. Section 5 compares monthly mean near-surface temperature, winds, precipitation, soil moisture, and evaporation. Section 6 presents an hourly scale comparison of near-surface temperature and winds. Section 7 compares the trends of near-surface temperature, 500-hPa height, and precipitation. Section 8 focuses on a major storm event and compares the water budgets. These 4 sections (5 - 8) are designed to demonstrate the uncertainties in the regional analyses that resulted from differences in the systems. Section 9 concludes the paper.

2. Difference in large-scale analysis

Before comparing the CaRD10 and NARR regional scale analyses in detail, we will first examine the difference in the large-scale component of the two analyses. The difference can be significant since the observations used in these two analyses are very different, as discussed in the previous section. CaRD10 is simply forced by large-scale analysis without directly

assimilating observations, so examination of the difference in large scale analysis is important. If the large-scale analyses between CaRD10 and NARR are very different, we can never expect CaRD10 to be similar to NARR. For this comparison, we used 500-hPa height and 200-hPa wind fields as “large-scale analysis,” since small scale features appearing near the surface are sufficiently damped and only large-scale features remain at these levels. Here we define “large-scale” as a scale greater than 1000 km, which is used as a critical scale for the wind to be forced to global reanalysis in the scale selective bias correction method. The 1000 km scale for the CaRD10 domain of approximately 1600 km x 2000 km implies a wave with one positive and one negative peak and a node at the center in both x- and y- directions.

The root mean square differences (RMSD) of daily 500-hPa height analyses averaged for winter (DJF) and summer (JJA), 2001 and 2002 over the CaRD10 domain, 8.2 m and 7.0 m respectively, are of about the same magnitude as the observational error of radiosonde (Xu et al 2000). The maximum difference of winter and summer mean 500-hPa height between CaRD10 and NARR for the period 1979-2002 is about 4 meters. These comparisons clearly indicate that the “large-scale analyses” between CaRD10 and NARR are close enough to produce similar climate analyses. A similar comparison of upper level daily wind showed that the RMSD at 200-hPa is about 3 m s^{-1} in both seasons, which is the same level as the observational error. The comparison of the fit to selected radiosonde winds showed that NARR RMSD is 1-2 m s^{-1} less than that of CaRD10. With the similarities and differences as stated, we consider the large scales of the CaRD10 and NARR sufficiently close to enable CaRD10 to improve upon a variety of small scale features requiring resolution significantly higher than that of the NARR.

3. Fit to station observations

In the next two sections we will focus on the efficacy of the regional downscaling and the importance of horizontal resolution. Table 1 is the comparison of correlation and RMSE of daily mean winds at 15 buoy observations (see Figure 1 and Table 2a of Part 1) along the California coast during January and August, 2000. Over the ocean, NARR winds fit better than CaRD10 to buoy observations on the average of all stations, but at some individual stations CaRD10 fits better than NARR does. Those stations are generally located on the lee side of the capes (for example, b14, b25, and b26). Station b25 in particular is known for the large day-to-day variability of winds due to the formation of mesoscale eddies (Catalina eddy; see section 4.1). The RMSE is smaller in NARR than CaRD10 at most stations. The assimilation of buoy winds in NARR apparently made the analysis fit better to observations where small scale features do not dominate, but the higher horizontal resolution of CaRD10 without the use of observations has a small advantage over NARR where variability is large.

This advantage of high spatial resolution is more apparent in the wind analysis over land where the effect of small scale topography dominates. Table 2 is the comparison of correlation and RMSE of daily mean winds at 12 airport stations (see Figure 1 and Table 2c of Part 1) in California for January and August, 2000. The CaRD10 fits better than NARR at most stations in terms of both correlation and RMSE, implying that detailed topography is essential for regional analysis over land even though these stations are located in relatively flat open areas. Surface wind observations are assimilated in NARR, but the additional information over land seems to be of limited benefit, partly due to its coarse resolution topography..

Table 3 presents the comparison of the correlation of daily mean temperature at the same stations as those of the wind verification over land. On all station average, CaRD10 is better in correlation and bias but worse in RMSE than NARR. At individual stations, neither CaRD10 nor

NARR stand out in terms of correlation. RMSE (mean bias is removed) is smaller in NARR than CaRD10 in August, but January performance is similar in both. The most notable difference between the two analyses is found in bias. The CaRD10 bias is smaller than NARR at most stations. For the bias comparison, temperature is corrected for elevation with a lapse rate of 6.5 K km^{-1} , so the elevation difference explains only a small part of the bias. CaRD10's surface topography and finer resolution land surface characteristics must have kept its bias small. In January the same four stations have a negative bias in CaRD10 and NARR, suggesting a common systematic error in both analyses for this month. In August both analyses have two to three times larger bias on all station average than in January, but the same stations do not necessarily result in a bias of the same direction.

4. Synoptic events

4.1 Catalina Eddy

When northerly winds cross the Transverse Ranges and descend over Santa Catalina Island, rapid warming of the air mass forms a low pressure center. This warm low pressure offshore of Santa Barbara and Los Angeles, south of Point Conception, draws marine air along the coast from the south and creates the eddy around the low pressure (Wakimoto 1987; Mass and Albright 1989). CaRD10 is able to produce well-defined eddies with strong winds and small-scale structures (Figure 5 of Part 1). On the contrary, NARR produces a weak eddy without much small-scale structure (Figure 2). The horizontal resolution is apparently important for the reproduction of mesoscale eddies, although the detailed verification requires observation.

4.2 Coastally Trapped Wind Reversal

When northerly winds along the coastline change direction and head north, this is called Coastally Trapped Wind Reversals (CTWR). CTWRs typically occur along mountainous

coastlines where cold upwelling results in a marine boundary layer capped by a strong inversion (Nuss et al. 2000; hereafter referred to as N2000). Figure 3 shows the evolution of a CTWR event from 18 UTC 21 July to 18 UTC 22 July 1996 from CaRD10 and NARR. This is a highly forced situation of a CTWR, chosen from N2000, for which the authors objectively analyzed and predicted streamlines of surface winds from COAMPS (Coupled Ocean/Atmospheric Mesoscale Prediction System; their Figure 14). Both CaRD10 and NARR show similar streamlines at 18 UTC 21 July in agreement with N2000. At 00 UTC 22 July, although not as large as N2000, the two analyses show a developed wind disturbance. By 18 UTC 22 July CTWR is well established both in CaRD10 and NARR. NARR's center is located farther south than N2000 and CaRD10, but the wind reversal is very well defined. NARR's 32 km seems to be sufficient for resolving a CTWR of this scale and forcing. CaRD10's streamlines show a more complex structure than N2000 and NARR, although it is not possible to say such a structure is real without observations.

4.3 Santa Ana Winds

When a slow moving high pressure system intensifies over the northern Midwest during winter, southern California often experiences strong, dry, warm northeasterly winds blowing from the desert region in eastern California/western Nevada towards the Pacific coast. This is one of the extreme events that define the "weather" in California. Figure 4 shows an example of a very strong Santa Ana event at 00 UTC 26 October 2003, when many parts of southern California experienced wildfires (Cedar fire; Keely et al. 2004). 2 m temperature anomalies from each analysis's 00 UTC October 2003 mean and full field 10 m winds are plotted. NARR shows only a modest positive temperature anomaly (up to 4 degrees Celsius) along the coastal areas of Southern California as opposed to 10 degrees or more in CaRD10, which is more realistic and fits better to observation. Both analyses show a similar northeasterly flow over land,

but the winds in CaRD10 are stronger. The two analyses differ in the wind pattern offshore of Los Angeles and San Diego. CaRD10 shows a complex wind response with northeasterly winds extending more into the coastal ocean area while NARR shows only consistent northwesterly winds over the same area.

5. Monthly Mean Comparisons

In the next 4 sections we will compare CaRD10 and NARR without referring to the station observations. Since surface observation density is limited even over land, it is not possible to verify the small differences between CaRD10 and NARR. The differences found in these comparisons can be interpreted as uncertainties in regional analyses due to differences in the analysis systems.

5.1 Near-surface Temperature

Figure 5 shows the difference in monthly mean temperature for the period from 1979 to 2002 at 2 m above ground between CaRD10 and NARR, after adjusting for the elevation difference with a lapse rate of 6.5 K km^{-1} . In January the NARR temperature is generally warmer than CaRD10 over most of the domain, mainly due to the smoother topography used in NARR, even after the elevation correction. CaRD10 is warmer than NARR over the mountains where the two analyses have different surface heights. Over the ocean in July CaRD10 is warmer than NARR, due to the use of different SST sources (monthly mean HadISST prior to 1981, and weekly NCEP 2DVAR SST after 1982 for CaRD10 [Fiorino 2004] and reconstructed SST [Smith and Reynolds 2003] prior to 1981, and Reynolds SST after 1982 for NARR [Reynolds et al 2002]). The land temperature in CaRD10 is colder than NARR and the geographical pattern is similar to that of January. The temperature difference is generally larger in July than in January. Several areas along the coastline show CaRD10 is colder in January and warmer in July, and the

differences are consistent with ocean temperature differences in these respective months. These coastal locations seem to be significantly influenced by offshore sea surface temperature, and the accuracy of the SST seems to be important for better land surface temperature analysis. CaRD10 shows more low cloud cover than NARR in July, when marine stratus is known to affect the coastal climate of California. However, near-surface temperatures at stations in the coastal area (CQT, LAX, LGB, SAN, SFO, and SMX in Table 3) do not indicate which regional analysis tends to fit better to observations, so the effect of marine stratus in coastal climate analysis is not clear.

5.2 Surface Winds

Figure 6 compares monthly mean winds over land at 10 m above ground between CaRD10 and NARR. For CaRD10, only one in three grid cells is plotted to match the NARR resolution. In January NARR produces little variation in speed and direction over most of the domain except in the north. In contrast, CaRD10 shows a detailed spatial pattern of winds that follow the complex terrain of California. The southwesterly in the Central Valley that accelerates over the Sierra Nevada is particularly clear in CaRD10. In the Southern California coast CaRD10 shows strong offshore winds which are absent in NARR. Our preliminary study showed that this wind is closely related to the occurrence of Santa Ana events (see also section 4.3) which are strong enough to appear in monthly averaged climatology.

In July, the wind pattern is similar between the two analyses but differences are again seen in the small-scale features. In NARR winds flow through the San Francisco Bay into the valley and branch to the north and south. The south branch continues further inland through the south end of the Sierra Nevada Range and changes direction towards the north, forming a trough-like feature. In CaRD10 similar wind flows are found, but they are broken into several regimes

due to the more complex topography in CaRD10. These differences in July wind pattern will be revisited in the diurnal variation discussion (section 6.2).

One significant shortcoming of CaRD10 is the absence of a southerly monsoon flow through the Gulf of California during summer (Mo et al. 2005). The southerly in the southern half of Nevada is also very weak in CaRD10. This is because the monsoon area is close to the southeastern corner of the CaRD10 domain and the coarse horizontal resolution of NNR does not resolve the small-scale monsoonal southerly jet along the Sierra Madre Occidental.

5.3 Precipitation and surface hydrology

CaRD10 has a positive precipitation bias as discussed in Part 1, which is apparent in comparison with NARR in January climatology (1979-2002; Figure 7). NARR assimilates precipitation observations, so its precipitation amount and spatial distribution is close to observations. Area-mean January precipitation is 2.82 mm day^{-1} in CaRD10 and 1.96 mm day^{-1} in NARR. CaRD10 produces twice as much precipitation as NARR in some heavy precipitation areas. Despite the positive bias, the spatial pattern of precipitation is similar in NARR and CaRD10. Note that CaRD10 shows much finer scale precipitation patterns over the Sierras.

A couple of other variables related to surface hydrology were compared between CaRD10 and NARR. Soil moisture (not shown) is a quantity that is strongly dependent on land model and precipitation forcing. The different land models used in CaRD10 and NARR (OSU scheme and Noah scheme, respectively) and the use of model precipitation in CaRD10 and observed precipitation in NARR resulted in very different soil moisture distributions. NARR does not show small-scale detail in soil moisture due to its coarser resolution, and also possibly to the coarser resolution of the observed precipitation ($1/8$ degree original data) remapped to its model grid. In general, the broader scale soil moisture fields in both seasons are very different in

CaRD10 and NARR. Without observation of soil moisture it is difficult to judge the quality of soil moisture. The differences in land model response to different land surface parameterizations under the same forcing are documented in Henderson-Sellers et al (1996).

The pattern of January latent heat flux (not shown) resembles that of soil moisture. The increased evaporation over the Sierras can be seen on both analyses, but it is much stronger in CaRD10. The evaporation is also much larger along the Northern California and Southern Oregon coast. Over the ocean, CaRD10 produces a particularly large evaporation south of Point Conception off the shore of Santa Barbara. The July latent heat flux pattern reflects the distribution of soil moisture in CaRD10, but this is not the case with NARR. Overall, the latent heat flux patterns are more similar to each other than the soil moisture patterns. Since atmosphere-land surface interaction takes place through evaporation and sensible heat flux, and not directly through soil moisture, this result is a little more reassuring from an atmospheric analysis point of view.

6. Hourly Scale Comparisons

6.1 Near-surface Temperature

CaRD10 produces outputs hourly but NARR produces outputs 3-hourly, therefore, 3-hourly output from CaRD10 is used for comparison. July 2 m temperature climatology of diurnal variation (for the period from 1979 to 2002) is shown in Figure 8. CaRD10 produces colder 2 m temperature than NARR throughout the day, but the diurnal variations between the two are very similar in pattern, except for the smaller scale features in CaRD10. There are some differences, though. For example, CaRD10 has two maxima in the northern and southern Central Valley, which are a couple of degrees warmer than the rest of the Valley, while NARR shows only one maximum in the southern Valley (Figure 8 a, b and h). These small scale differences

over the nearly flat Central Valley may be due to the finer resolution of CaRD10, which resolved the small-scale wind pattern and consequently determined the small-scale feature in near-surface temperature.

6.2 Surface Winds

Figure 9a shows the July 10 m wind comparison at 00 UTC (local afternoon). The two analyses produce quite similar wind patterns at this time. On the other hand, at 06 UTC (local nighttime), the two analyses differ greatly. The NARR wind flows from the San Francisco Bay into the valley and heads east at 35 to 36 N, and then north, forming a trough-like pattern across Southern California and Nevada. In the CaRD10 analysis, the inflow from the San Francisco Bay and the westerlies at 35-36N are different flow systems separated by the Tehachapi Mountains that bound the southern end of the Central Valley. A similar separation of the wind system is observed over Northern California, Southern Oregon and Northeastern Nevada, where CaRD10 shows small-scale systems of wind patterns.

The winds over the Gulf of California are very different, particularly at 06 UTC, between CaRD10 and NARR. This is due to the placement of the lateral boundary in CaRD10 (section 5.2).

7. Trends

7.1 Near-surface Temperature

Although the NARR period of 1979 to present is too short for a robust trend analysis, many papers have been published (e.g., Hurrell and Trenberth, 1998; Santer et al., 2000; Santer et al. 2003; Bengtsson et al., 2004; Simmons et al., 2004; Agudelo and Curry, 2004; Chase et al., 2000) to examine the recent temperature trend since 1979, when the Microwave Sounding Unit satellite measurements became available. Therefore, it is of great interest to compare CaRD10

and NARR in the last quarter of a century to understand the climate trend in regional analyses. The trends presented in this section are computed by the least square linear regression. Except for very large trend signal, most trend is not significantly different from zero (95 % statistical confidence), but the spatial pattern of trend will be informative for understanding the different responses of regional analysis to changes in large-scale atmospheric analysis over time. Therefore, particular focus is placed on the geographical pattern of trends of relative magnitude within the same analysis, and the comparison of such spatial patterns between the two analyses.

Figure 10a shows the comparison of DJF near-surface temperature trend from 1979 to 2002. Coastal and low elevation valley areas do not show strong trend. CaRD10 produces a negative trend on the windward side of the Sierra Nevada and a positive trend on the lee side and most of Nevada. A positive trend is also prevalent for inland southern California and northern Nevada. NARR shows a positive trend only in the east and the west sides of Lake Tahoe and it shows a negative trend over the Sierra Nevada and northern Nevada. The rest of the domain shows little trend. Thus, the two analyses are very different in the spatial pattern. During JJA 2 m temperature trend shows a negative trend in the southern California coastal areas in both analyses (Figure 10b). The trend is also positive in Northern California in both analyses, but a particularly large positive trend over the northern Central Valley in NARR is replaced by a near zero trend in CaRD10. The eastern half of the domain shows a positive trend in CaRD10 but only a small positive trend in NARR. In fact, the difference between the two analyses in each season is much larger than the difference between two seasons in each analysis.

7.2 500-hPa height

The trend in 2 m temperature can be partitioned into the trend in large-scale circulation and in local scale. In order to understand the trend in large-scale, we examined the trend in 500-

hPa geopotential height. Figure 11 shows the change in 500-hPa height from 1979 to 2002 from the trend of the height at each grid point. In DJF, there is a gradient of height trend from a negative trend in the northwest corner to a positive trend in the southeast corner in both analyses. In JJA, the entire domain shows a positive trend for both CaRD10 and NARR, but with somewhat different magnitude, and the gradient has been reversed from DJF but the patterns are again very similar. Thus for both seasons, CaRD10 and NARR show very similar patterns in the 500-hPa height trend indicating that the trends in the large-scale analysis between the two are similar.

An interesting finding is that the northwest-southeast gradient found in the 500-hPa height trend is not seen in the near-surface temperature trend, thus the trend in large-scale (such as the global effect of green house gasses) does not seem to be directly correlated to the trend in near-surface temperature. Therefore, the large difference in near-surface trend between the two analyses is due to differences in near-surface processes, most likely to land surface conditions and to radiation fluxes reaching the surface.

7.3 Precipitation

Although 2 m temperature trends show different spatial patterns, the precipitation trend is consistent between the two analyses (Figure 10c). DJF precipitation increases in the northwest where large precipitation is produced in both CaRD10 and NARR. Another common pattern found in both analyses is a precipitation decrease on the lee side of the Sierras. The rest of the domain with only moderate amounts of precipitation shows little trend. Considering that the CaRD10 precipitation is model produced, it is quite comforting to find that the low frequency variability of precipitation is well reproduced. This agreement between the two analyses also

suggests that the precipitation trend is determined mainly by the trend in large scale and less by the trend in near-surface fields.

8. Water Budgets

In order to demonstrate the uncertainties associated with regional analyses in a quantitative way, we present an example of a water budget study for a major storm event in California selected from strong atmospheric river events (Ralph et al 2004). Plots are made for the mean of the three-day event (Nov 7 to 9, 2002). We separated the water budgets into three areas by the amount of precipitation (Figure 12a). Area A is the middle of the domain where most precipitation occurs (35-41N and 118-122W) and CaRD10 produces more precipitation (30.4 mm day^{-1}) than NARR (24.0 mm day^{-1}). Area B is in the northwest corner of the domain where moderate precipitation is found (41-45N and 122-126W) and CaRD10 has less precipitation (16.4 mm day^{-1}) than NARR (21.7 mm day^{-1}). Area C is to the west of the domain A (35-41N and 122-126W) and the precipitation amount is not very different in the two analyses (14.1 mm day^{-1} for CaRD10 and 12.4 mm day^{-1} for NARR). Table 4 summarizes the area averaged quantities of hydrological variables. We observe that over area A, where the precipitation is overestimated by CaRD10, the moisture convergence is much larger than in NARR (Figure 12b). In other areas with moderate precipitation, the CaRD10 moisture convergence is about the same as that of the NARR, suggesting that the moisture convergence is the reason for the overestimation of precipitation in CaRD10, although we cannot determine whether this is the result or the cause. Another feature of CaRD10 that favors moisture convergence in area A is the wind pattern (Figure 12e). A 10 m wind comparison suggests that CaRD10 produces a consistent wind pattern (southwesterly) from the valley that is perpendicular to the mountain ranges. Less southerly wind is found in CaRD10 than NARR that escapes

without producing orographic precipitation. The extra moisture that enters area A is brought into the domain by a large moisture flux in the southwest corner of the domain (Figure 12c). Slightly larger precipitable water over the ocean accounts for the larger moisture flux in CaRD10 than in NARR (Figure 12d). However, the domain average precipitable water is about the same in the two analyses. The spatial pattern and gradient of precipitable water and the direction of winds make a difference in the water budgets for the storm event between the two analyses.

One curious finding is that the NARR moisture convergence is less than precipitation for areas A and B, and even the addition of the evaporation cannot fill in the difference (Table 4). In these areas, the systems require a large artificial moisture source or a decrease in local precipitable water to explain the precipitation, which seems somewhat unrealistic. Whether this is the result of using observed precipitation to force model dependent variables is an interesting question to be studied.

Table 4 shows the residual term calculated from precipitation, evaporation, moisture convergence, and changes in precipitable water. CaRD10 and NARR show residuals of similar size, suggesting the two analyses have similar hydrological budget study uncertainties.

9. Summary and Conclusions

This paper is the second part of a two-part paper and it compares the dynamically downscaled reanalysis (CaRD10) with North American Regional Reanalysis. There are several fundamental differences in the basic system design between CaRD10 and NARR. The CaRD10 forces the high resolution regional model with coarse resolution global reanalysis without injecting any observations, but uses the scale selective bias correction to maintain the large scale part of the reanalysis. It ran with 10 km resolution, hourly output from 1948 to present. NARR

is based on state-of-the-art 3-dimensional variational analysis, using surface and high density satellite raw radiance observations. NARR also assimilates observed precipitation. The NARR analysis system ran with 32 km resolution, 3-hourly output from 1979 to present. The numerics and the physical processes included in the two models are also different. This paper compared the two analyses, documented the efficacy of regional downscaling and the importance of horizontal resolution, and estimated the uncertainties in the high-resolution regional analyses.

CaRD10 is forced by NNR, while NARR uses a different analysis system including new and additional datasets. However, the difference in the large-scale analysis (the scale greater than 1000 km) examined from 500-hPa height and 200-hPa wind confirms that the large-scale analyses between CaRD10 and NARR are very similar.

The comparison of the fit of the daily wind analyses to near-surface observation showed that over ocean, CaRD10 fits better than NARR where the daily variability is large, while over land, CaRD10 generally fits better than NARR. Daily near-surface temperature correlation with observation shows a similar skill in CaRD10 and NARR. CaRD10 shows a much smaller bias compared to NARR, but NARR produces smaller RMSE than CaRD10.

Several synoptic examples are presented to highlight how different topography and spatial resolution affect the local climate. The Catalina Eddy is seen very well in CaRD10 with many mesoscale features, when NARR shows weak winds. Coastally Trapped Wind Reversal is well simulated both in CaRD10 and NARR, but CaRD10 shows more complex structure of wind disturbance. Santa Ana winds are produced well in both CaRD10 and NARR, but temperature anomaly is much greater in CaRD10 than NARR.

From the fit of the analysis to near-surface observation and examination of a few cases of regional meso-scale events, the horizontal resolution of the model seems to have a large

impact, and the data assimilation in NARR does not seem to use the near-surface observation as effectively as desired.

A comparison of the monthly climatology between the two analyses showed that the CaRD10 near-surface temperature and winds are very similar to NARR with more regional detail, especially in winter. During the summer, CaRD10 winds associated with the Southwestern monsoon and the Gulf of California low level jet are poor due to the placement of the lateral boundary. CaRD10 has a positive bias in precipitation compared to NARR, which uses observations, but the spatial patterns of the two are similar and CaRD10 shows small-scale details, especially over the mountains. The spatial pattern of latent heat flux reflects that of soil moisture, but the two analyses show better agreement for latent heat flux than for soil moisture.

The diurnal cycle of near-surface temperature is similar in CaRD10 and NARR but CaRD10 is generally colder. CaRD10 shows spatially detailed patterns of temperature diurnal variation in the Central Valley and the Sierra Nevada. The two surface winds analyses generally agree with each other but more differences are apparent during nighttime, when winds are generally weak. The winds from the San Francisco Bay through the Central Valley and from south of the Sierras into the higher Nevada plains show dissimilarities due to differences in resolving small scale topography.

The near-surface temperature trends from 1979 to 2002 do not produce consistent spatial patterns between the two analyses. Some common features are a small negative trend in the Southern California coastal region and a positive trend in Northern California during summer. In fact, summer and winter trends in each analysis are more similar than trends in the same season between the two analyses. Large-scale field trend as represented by 500-hPa geopotential height shows a similar northwest-southeast gradient in CaRD10 and NARR in both seasons. Such a

spatial pattern is little-seen in near-surface temperature trend. The surface climate trend seems to be more influenced by regional topography, model physics and land surface schemes. However, the winter precipitation trend is similar in the two analyses. There is a positive trend in the area with large precipitation and a decreasing trend on the lee side of the Sierras. The rest of the domain shows little trend. This suggests that the precipitation trend is more influenced by the trend in large scale circulation.

In a major three-day storm event, CaRD10 produces more precipitation than NARR in the area mean. Most precipitation positive bias comes from the mountain areas where heavy precipitation is observed. The path of precipitable water into Southern California is narrower and carries more water vapor in CaRD10 than NARR, although the area mean precipitable water is the same. Larger moisture flux due to the precipitable water spatial distribution brings extra moisture over land towards the mountains. The wind direction in CaRD10 is southwesterly and perpendicular to the mountain ranges that favor precipitation. As a result, CaRD10 produces more precipitation than NARR. The moisture budget calculation showed that both analyses suffer from a budget residual that cannot be ignored. In this regard, both analyses have a similar uncertainty for water budget study.

Overall, CaRD10 shows a fairly good agreement with the NARR. On many occasions, CaRD10 benefits from higher spatial resolution and fine-scale topography. CaRD10's higher temporal output frequency also aids more detailed diagnostics. The lack of assimilated observation is outweighed by finer spatial resolution in many cases. In NARR, the current data assimilation system is not able to properly assimilate surface observations. The use of balance equation without the consideration of friction as a constraint in the system, and the use of

homogeneous guess and observation error are some of the known problems that affect efficient use of the near-surface observations (D. Parrish, personal communication, 2006).

Dynamical downscaling forced by a global analysis is a computationally economical approach to regional scale long term climate analysis and can provide a high quality climate analysis comparable to data assimilated regional reanalysis.

However, the uncertainties of analysis can be very large, depending on the fields of interest and the diagnostic calculations (such as trend and water budget studies). Users of the regional analyses should be aware of these uncertainties when utilizing them for their own research.

Acknowledgements

This work was funded by the California Energy Commission Public Interest Energy Research (PIER) program, which supports the California Climate Change Center (Award Number MGC-04-04). The authors sincerely thank G. Franco for his assistance in performing this research. We would also like to thank Dr. Dan Cayan for continuous encouragement throughout this study. The computations were performed at the National Center for Atmospheric Research, the San Diego Supercomputer Center and the University of Illinois Super Computing Center. The assistance of Ms. Diane Boomer in refining the writing is appreciated. Three anonymous reviewers helped to improve the manuscript.

References

- Agudelo, P.A. and J. Curry, 2004: Analysis of spatial distribution in tropospheric temperature trends, *Geophys. Res. Lett.*, **31**,L22207, doi:10.1029/2004GL020818.
- Bengtsson, L., S. Hagemann, K.I. Hodges, 2004: Can climate trends be calculated from reanalysis data?, *J. Geophys. Res.*, **109**, D11111, doi:10.1029/2004JD004536.
- Bromwich, D.H. and R.L. Fogt, 2004: Strong trends in the skill of the ERA-40 and NCEP-NCAR Reanalyses in the High and Midlatitudes of the Southern Hemisphere, 1958-2001. *J. Climate*, **17**, 4603-4619.
- Chase, T.N., R.A. Pielke Sr., J.A. Knaff, T.G.F. Kittel, and J.L. Eastman, 2000: A Comparison of Regional Trends in 1979-1997 Depth-averaged tropospheric Temperatures. *Int. J. Climatology*, **20**, 503-518.
- Daly, C., R.P. Neilson, and D.L. Phillips, 1994: A Statistical-Topographic Model for Mapping Climatological Precipitation over Mountainous Terrain. *J. Appl. Meteor.*, **33**,140–158.
- Daly, C., G. H. Taylor, W.P. Gibson, T.W. Parzybok, G.L. Johnsonn, and P. Pasteris, 2001: High-quality spatial climate data sets for the United States and beyond. *Transactions of the American Society of Agricultural Engineers*, **43**, 1957–1962.
- Daly, C., W.P. Gibson, G.H. Taylor, G.L. Johnson, and P. Pasteris, 2002: A knowledge-based approach to the statistical mapping of climate. *Climate Research*, **22**, 99–113.
- Fiorino, M., 2004: A Multi-decadal Daily Sea Surface Temperature and Sea Ice Concentration Data Set for the ERA-40 Reanalysis. ERA-40 project Report Series. ECMWF, Shinfield Park, Reading, RG2 9AX, UK. 16pp.
- Gibson, J. K., P. Kallberg, S. Uppala, A. Nomura, A. Hernandez, E. Serrano, 1997: ERA Description, ECMWF Re-Analysis Final Report Series, 1, 71pp. ECMWF, Reading, UK.

- Henderson-Sellers, A., K. McGuffie and A. J. Pitman, 1996: The project for intercomparison of land-surface parameterization schemes (PILPS): 1992 to 1995. *Climate Dynamics*, **12**, 849-859.
- Higgins, R. W., W. Shi, E. Yarosh and R. Joyce, 2000: Improved United States precipitation Quality control system and analysis. NCEP/Climate Prediction Center Atlas No. 7, U.S. Department of Commerce. [Available at: http://www.cpc.mcep.npoaa.gov/research_papers/ncep_cpc_atlas/7/index.html]
- Hodges, K.I., B.J. Hoskins, J. Boyle, and C. Thorncroft, 2003: A comparison of recent reanalysis datasets using objective feature tracking: storm tracks and tropical easterly waves. *Mon. Wea. Rev.*, **131**, 2012-2037.
- Hurrell J. W. and K. E. Trenberth, 1998: Difficulties in Obtaining Reliable Temperature Trends: Reconciling the Surface and Satellite Microwave Sounding Unit Records. *J. Climate*, **11**, 945-967.
- Kain, J.S., and J.M. Fritsch, 1993: Convective parameterization for mesoscale models: The Kain-Fritsch scheme. The representation of cumulus convection in numerical models. *Meteor. Monogr.*, No. 24, Amer. Meteor. Soc., 165-170.
- Kalnay, E., and Coauthors, 1996: The NCEP/NCAR 40-year reanalysis project. *Bull. Amer. Meteor. Soc.*, **77**, 437-471.
- Kanamaru, H. and M. Kanamitsu, 2007: Scale Selective Bias Correction in a Downscaling of Global Analysis Using a Regional Model. *Mon. Wea. Rev.*, **135**, 334-350.
- Kanamitsu, M. and H. Kanamaru, 2006: 57-year California Reanalysis Downscaling at 10 km (CaRD10) – Part 1. System Detail and Validation with Observations --. *J. Climate*, (submitted).

- Kanamitsu, M., W. Ebisuzaki, J. Woolen, J. Potter, and M. Fiorino, 2002: NCEP/DOE AMIP-II Reanalysis (R-2). *Bull. Amer. Meteor. Soc.*, **83**, 1631-1643.
- Keely, J. E., C. J. Fotheringham and M. Moritz, 2004: Lessons from the October 2003 Wildfires in Southern California. *J. Forestry*, **102**, 26-31.
- Leung, L.R., Y. Qian, J. Han, and J.O. Roads, 2003: Intercomparison of global reanalyses and regional simulations of cold season water budgets in the Western United States. *J. Hydromet.*, **4**, 1067-1087.
- Mass, C. F. and M. D. Albright, 1989: Origin of the Catalina Eddy, *Mon. Wea. Rev.*, **117**, 2406-2436.
- Mesinger, F., and Coauthors, 2006: NORTH AMERICAN REGIONAL REANALYSIS. *Bull. Amer. Met. Soc.* **87**, 343-360.
- Mo, K.C., M. Chelliah, M.L. Carrera, R.W. Higgins, W. Ebisuzaki, 2005: Atmospheric moisture transport over the United States and Mexico as evaluated in the NCEP regional reanalysis. *J. Hydromet.*, **6**, 710-728.
- Nuss, W. A., and Coauthors, 2000: Coastally Trapped Wind Reversals: Progress toward Understanding. *Bull. Amer. Met. Soc.*, **81**, 719-743.
- Ralph, F. M., P. J. Neiman and G. A. Wick, 2004: Satellite and CALJET aircraft observations of atmospheric rivers over the eastern North-Pacific Ocean during the winter of 1997/98. *Mon. Wea. Rev.*, **132**, 1721-1745.
- Reynolds, R. W., N. A. Rayner, T. M. Smith, D. C. Stokes and W. Wang, 2002: An improved in situ and satellite SST analysis for climate. *J. Climate*, **15**, 1609-1625.

- Ruiz-Barradas, A. and S. Nigam, 2005: Warm season rainfall variability over the U.S. Great Plains in observations, NCEP and ERA-40 reanalyses, and NCAR and NASA atmospheric model simulations. *J. Climate*, **18**, 1808-1830.
- Santer, B. D., and Coauthors, 2000: Interpreting Differential Temperature Trends at the Surface and in the Lower Troposphere. *Science*, **287**, 1227-1232.
- Santer, B.D., and Coauthors, 2003: Contributions of Anthropogenic and Natural Forcing to Recent Tropopause Height Changes. *Science*, **301**, 479-483.
- Schubert, S., and Coauthors, 1995: A multi-year assimilation with GEOS-1 system: Overview and results. NASA Tech Rept Series on Global Modeling and Data Assimilation, Ed. M. J. Suarez, 6, 183pp.
- Simmons A. J., and J. K. Gibson, 2000: The ERA-40 Project Plan. ERA-40 Project Report Series. ECMWF, Shinfield Park, Reading, Berkshire, RG2 9AX, UK.
- Simmons, A.J., and Coauthors, 2004: Comparison of trends and low-frequency variability in CRU, ERA-40, and NCEP/NCAR analyses of surface air temperature. *J. Geophys. Res.*, **109**, D24115, doi:10.1029/2004JD005306.
- Smith, T.M., and R.W. Reynolds 2003: Extended reconstruction of global sea surface temperatures based on COADS data (1854-1997). *J. Climate*, **16**, 1495-1510.
- Sterl, A., 2004: On the (in) homogeneity of reanalysis products. *J. Climate*, **17**, 3866-3873.
- Trenberth, K.E., D.P. Stepaniak, and J.M. Caron, 2002: Accuracy of atmospheric energy budgets from analyses. *J. Climate*, **15**, 3343-3360.
- Trigo, I.F., 2006: Climatology and interannual variability of storm-tracks in the Euro-Atlantic sector: a comparison between ERA-40 and NCEP/NCAR Reanalyses. *Climate Dynamics*, **26**, 127-143.

- Uppala, S. M., and Coauthors, 2005: The ERA-40 re-analysis *Q. J. Royal Meteor. Soc.*, **131**, 2961-3012.
- Wakimoto, R. M., 1987: The Catalina Eddy and its Effect on Pollution over Southern California. *Mon. Wea. Rev.*, **115**, 837-855.
- Xu, Q., L. Wei, A. V. Tuyl and E. H. Barker, 2000: Estimation of Three-Dimensional Error Covariances. Part I: Analysis of Height Innovation Vectors. *Mon. Wea. Rev.*, **129**, 2126-2135.
- Zhao, Q. Y., and F. H. Carr, 1997: A prognostic cloud scheme for operational NWP models. *Mon. Wea. Rev.*, **125**, 1931- 1953.

Figure Captions

Figure 1 Surface height (m) in a) CaRD10, b) NARR and c) the difference between the two analyses.

Figure 2 A Catalina Eddy event in NARR at 1500UTC, May 22, 1984. Shades and arrows indicate winds at 10m above surface (m s^{-1}). The CaRD10 plot of the same event is presented as Figure 5 of Part 1.

Figure 3 Comparison of the evolution of Coastally Trapped Wind Reversal on 21-22 July 1996. Stream lines of 10 m winds are plotted. CaRD10 (left) and NARR (right). Top panels are 18 UTC 21 July, middle panels are 00 UTC 22 July, and bottom panels are 18 UTC 22 July.

Figure 4 Comparison of a Santa Ana event at 00 UTC 26 October 2003. Arrows are 10 m wind vectors (m s^{-1}). Shades are temperature anomaly (K) from each analysis's 00 UTC October 2003 mean.

Figure 5 2 m temperature difference (K) between CaRD10 and NARR in January and July.

Figure 6 Comparison of 10 m wind (m s^{-1}) between CaRD10 (left) and NARR (right) in January (top panels) and July (bottom panels).

Figure 7 Comparison of monthly mean precipitation rate (mm day^{-1}) between CaRD10 (left) and NARR (right) in January.

Figure 8 Comparison of diurnal variation of July 2 m temperature between CaRD10 (left) and NARR (right) at 3 hour intervals from 00 UTC to 21 UTC.

Figure 9 Comparison of July 10 m wind (m s^{-1}) between CaRD10 (left) and NARR (right) at 00 UTC (upper panels) and 06 UTC (lower panels).

Figure 10 Comparison of trend for the period 1979 to 2002 between CaRD10 (left) and NARR (right). a) 2 m temperature trend (K year^{-1}) in DJF, b) 2 m temperature trend (K year^{-1}) in JJA, and c) precipitation rate trend ($\text{m day}^{-1} \text{ year}^{-1}$) in DJF.

Figure 11 Comparison of 500-hPa height trend ($\text{m}/23\text{years}$) for the period 1979 to 2002 between CaRD10 (left) and NARR (right) in (a) DJF and (b) JJA.

Figure 12 Comparison of a storm event on 7-9 November 2002. Left column is CaRD10 and right column is NARR. (a) Precipitation (mm day^{-1}) (b) Moisture convergence (mm day^{-1}) (c) Vertically integrated moisture flux ($\text{kg m}^{-1} \text{ s}^{-1}$) (d) Precipitable water (kg m^{-2}), and (e) 10m wind (m s^{-1}). Superimposed are areas A to C for the water budget study.

Tables

Table 1 Vector anomaly correlation and RMSE of winds of two analyses and fifteen buoy observations during 2000. All vector correlations in the table are significant at 95 % level from bootstrap tests. When at least one of the scalar correlations (u, v winds, and wind speed) is different from its counterpart at 95 % significance level, better correlation is indicated in bold.

	January				August			
	Correlation		RMSE (m s ⁻¹)		Correlation		RMSE (m s ⁻¹)	
	CaRD10	NARR	CaRD10	NARR	CaRD10	NARR	CaRD10	NARR
b11	N/A	N/A	N/A	N/A	0.65	0.69	1.48	1.19
b12	N/A	N/A	N/A	N/A	0.68	0.68	1.98	1.67
b13	0.94	0.95	2.70	2.15	0.72	0.80	2.20	2.59
b14	0.89	0.88	2.69	2.14	0.78	0.70	1.88	1.86
b22	0.91	0.89	3.17	2.21	0.64	0.67	2.39	1.56
b23	0.73	0.89	3.89	2.82	0.69	0.67	1.73	1.47
b25	0.77	0.76	2.77	2.21	0.58	0.55	1.27	1.53
b26	0.92	0.91	2.48	2.71	0.83	0.75	1.36	2.94
b28	N/A	N/A	N/A	N/A	0.73	0.69	2.21	1.76
b42	0.88	0.93	3.16	2.09	0.69	0.68	1.88	1.62
b47	0.93	0.93	2.72	1.86	0.78	0.86	1.40	1.21
b53	0.69	0.70	2.52	2.45	0.54	0.62	2.35	1.79
b54	0.66	0.77	3.57	2.01	0.67	0.81	2.03	1.34
b62	0.85	0.85	2.71	1.95	0.68	0.68	1.61	1.28
b63	0.69	0.85	2.91	1.37	N/A	N/A	N/A	N/A
All station average	0.82	0.86	2.94	2.17	0.69	0.70	1.84	1.70

Table 2 Vector anomaly correlation and RMSE of winds of two analyses and twelve land station observations during 2000. All vector correlations in the table are significant at 95 % level from bootstrap tests. When at least one of the scalar correlations (u, v winds, and wind speed) is different from its counterpart at 95 % significance level, better correlation is indicated in bold.

	January				August			
	Correlation		RMSE (m s ⁻¹)		Correlation		RMSE (m s ⁻¹)	
	CaRD10	NARR	CaRD10	NARR	CaRD10	NARR	CaRD10	NARR
BFL	0.43	0.29	2.33	2.92	0.53	0.05	1.59	2.19
BIH	0.49	0.12	3.45	4.64	0.43	0.38	4.00	4.47
CQT	0.44	0.37	2.29	0.98	0.28	0.12	0.96	0.76
FAT	0.59	0.44	2.94	3.35	0.41	0.40	1.72	1.99
LAX	0.54	0.44	2.81	2.88	0.41	0.44	1.62	1.78
LGB	0.58	0.40	2.63	2.81	0.38	0.54	2.35	2.14
RDD	0.57	0.20	4.18	7.43	0.52	0.45	1.52	2.12
SAC	0.64	0.30	3.52	4.81	0.56	0.55	2.34	2.68
SAN	0.41	0.43	2.94	2.83	0.47	0.54	2.68	2.60
SCK	0.60	0.53	3.73	5.00	0.55	0.45	2.39	2.59
SFO	0.78	0.60	4.12	4.60	0.56	0.60	4.53	4.29
SMX	0.63	0.55	4.01	4.80	0.48	0.39	1.74	2.06
All station average	0.56	0.39	3.24	3.92	0.46	0.41	2.29	2.47

Table 3 Correlation, RMSE, and bias of daily mean temperature of two analyses and twelve land station observations during 2000. For the RMSE, mean value is subtracted at each station. For the bias, temperature is corrected for elevation with lapse rate of 6.5K km⁻¹ and absolute values of bias at each station are used for all-station average. Correlations that are not statistically significant at 95 % confidence level are in parentheses. When correlation is different from its counterpart at 95 % confidence level, better correlation is indicated in bold.

	January						August					
	Correlation		RMSE (K)		Bias (K)		Correlation		RMSE (K)		Bias (K)	
	C10	NARR	C10	NARR	C10	NARR	C10	NARR	C10	NARR	C10	NARR
BFL	0.83	0.78	1.84	2.05	0.53	2.86	0.90	0.89	1.25	1.37	-2.28	4.87
BIH	0.55	0.62	3.33	2.35	0.36	2.22	0.92	0.92	1.13	0.96	0.18	2.48
CQT	0.73	0.81	1.80	1.58	-0.08	-1.05	0.81	0.68	1.75	1.53	-0.41	-3.95
FAT	0.91	0.89	1.37	1.48	0.63	1.64	0.90	0.92	1.23	1.12	-2.33	3.00
LAX	0.74	0.82	1.68	1.50	-0.47	-0.92	0.59	0.61	2.01	1.01	0.22	-1.62
LGB	0.82	0.66	1.46	1.91	-0.88	-1.22	0.74	(0.14)	1.39	1.93	-2.67	-5.48
RDD	0.64	0.68	1.82	1.68	0.12	0.97	0.90	0.80	1.31	1.73	-1.10	2.67
SAC	0.86	0.73	1.09	1.56	0.56	0.44	0.81	0.82	1.76	1.61	-0.98	3.33
SAN	0.84	0.83	1.50	1.39	0.15	0.27	0.66	0.66	1.34	0.97	-1.04	1.10
SCK	0.83	0.82	1.20	1.38	0.34	0.34	0.86	0.88	1.50	1.30	-1.91	1.43
SFO	0.80	0.68	1.10	1.18	-1.06	-0.27	(0.26)	(0.54)	2.22	1.32	-0.37	-1.09
SMX	0.70	0.72	1.68	1.55	1.11	1.68	(0.14)	0.41	3.81	1.76	4.68	5.11
All station average	0.77	0.75	1.66	1.63	0.52	1.15	0.71	0.69	1.73	1.38	1.51	3.01

Table 4 Area-mean water budget on 7-9 November 2002. CONV is vertically integrated moisture convergence (mm day^{-1}), P is precipitation rate (mm day^{-1}), E is evapotranspiration (mm day^{-1}), ΔPWAT is precipitable water change from the 1st day to the 3rd day (mm day^{-1}), and Res is residual calculated as $\text{P}-\text{E}-\text{CONV}+\Delta\text{PWAT}$ (mm day^{-1}). Domains are: Whole (Entire domain in Figure 16 (31-45 N and 114-126W)), Area A (heavy precipitation area in the middle of the domain; 35-41N and 118-122W), Area B (northwest corner; 41-45N and 122-126W), and Area C (to the west of Area A; 35-41N and 122-126W).

Domain	Analyses	CONV	P	E	ΔPWAT	Res
Whole	CaRD10	13.4	11.1	0.9	1.6	-1.7
	NARR	9.0	9.7	0.5	1.2	1.4
A	CaRD10	32.7	30.4	1.5	2.1	-1.8
	NARR	18.2	24.0	0.6	2.1	7.2
B	CaRD10	17.2	16.4	2.3	-3.1	-6.1
	NARR	13.8	21.7	1.5	-2.4	4.0
C	CaRD10	13.0	14.1	0.3	-3.2	-2.4
	NARR	11.2	12.4	0.3	-2.6	-1.6

Figures

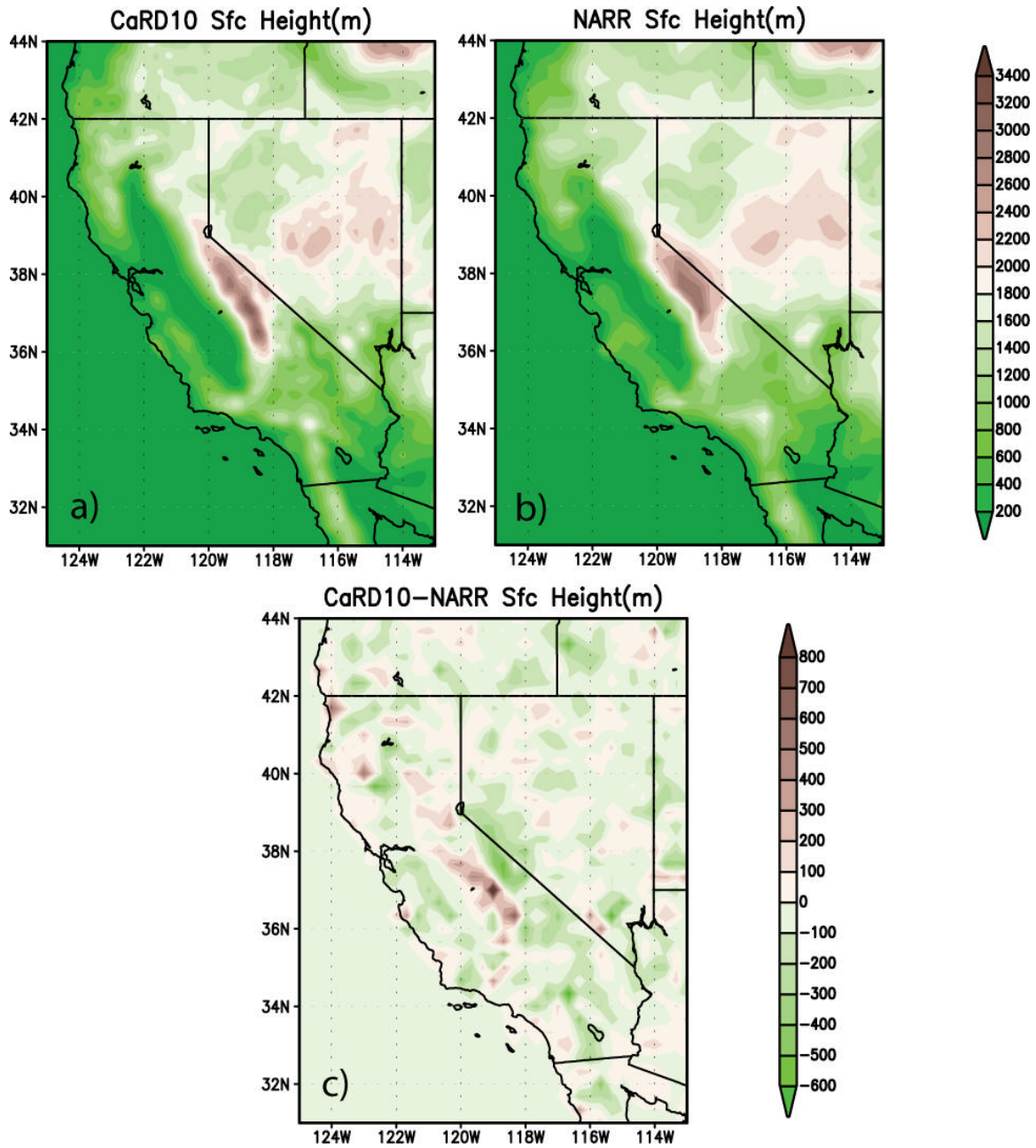


Figure 1 Surface height (m) in a) CaRD10, b) NARR and c) the difference between the two analyses.

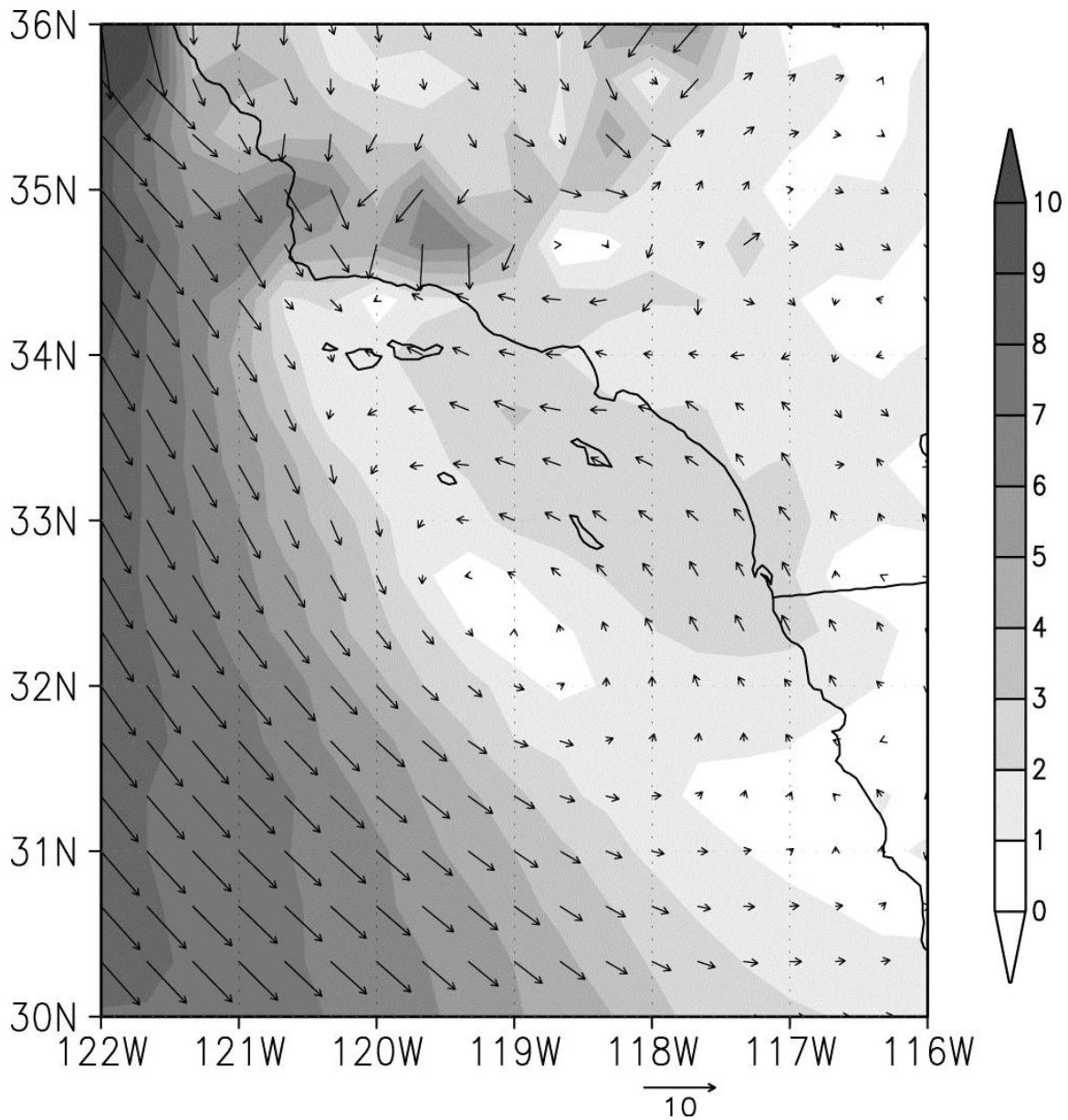


Figure 2 A Catalina Eddy event in NARR at 1500UTC, May 22, 1984. Shades and arrows indicate winds at 10m above surface (m s^{-1}). The CaRD10 plot of the same event is presented as Figure 5 of Part 1.

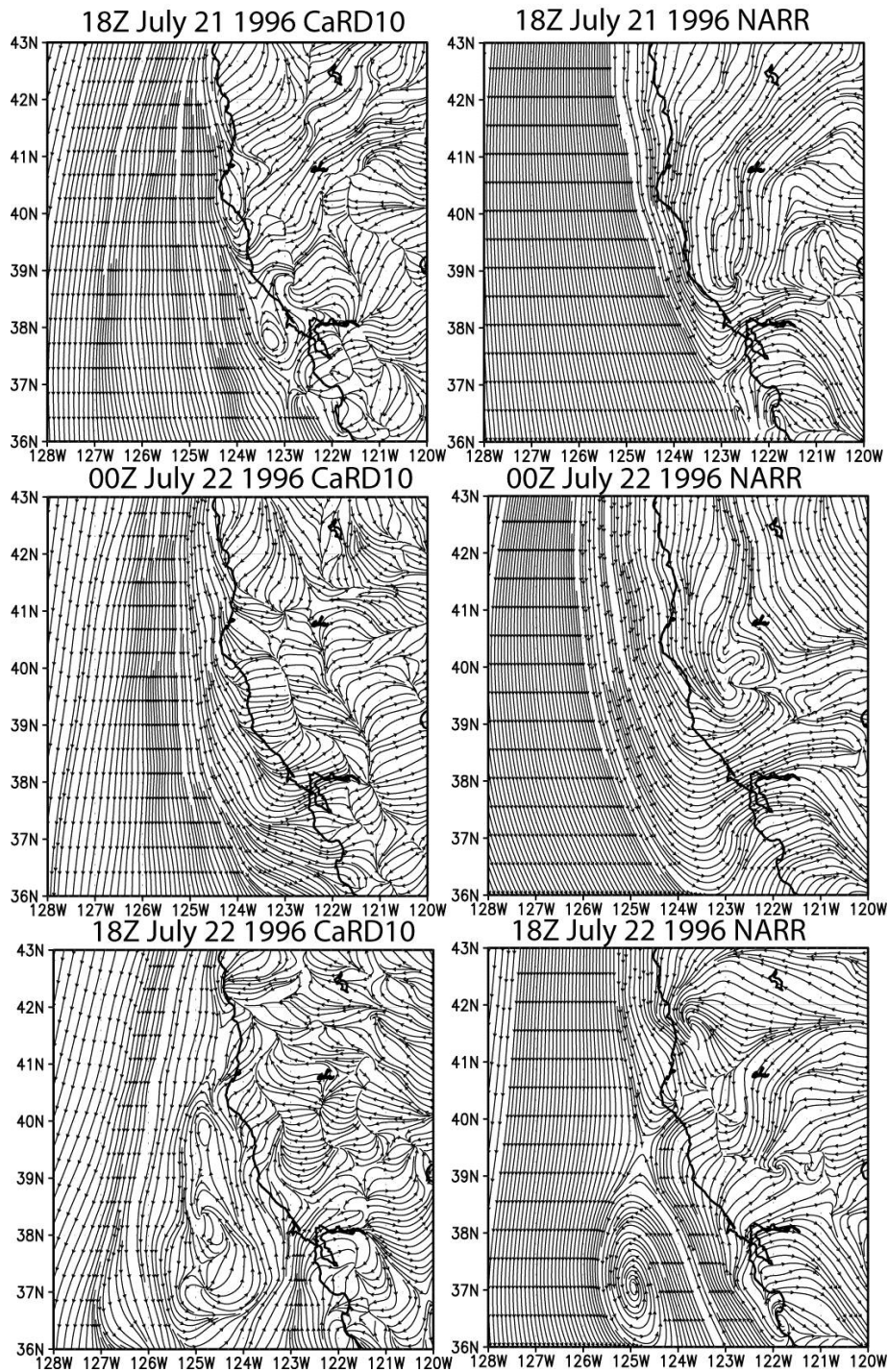


Figure 3 Comparison of the evolution of Coastally Trapped Wind Reversal on 21-22 July 1996. Stream lines of 10 m winds are plotted. CaRD10 (left) and NARR (right). Top panels are 18 UTC 21 July, middle panels are 00 UTC 22 July, and bottom panels are 18 UTC 22 July.

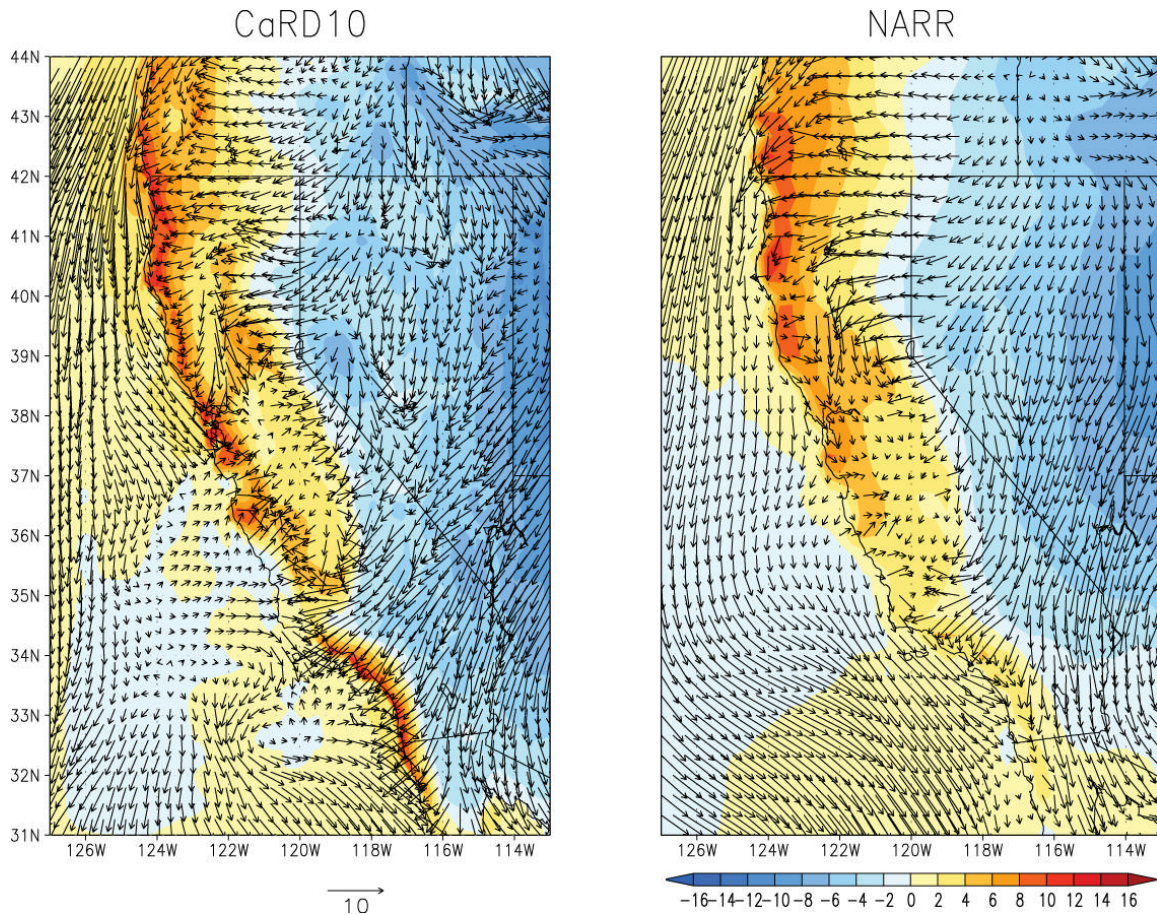


Figure 4 Comparison of a Santa Ana event at 00 UTC 26 October 2003. Arrows are 10 m wind vectors (m s^{-1}). Shades are temperature anomaly (K) from each analysis's 00 UTC October 2003 mean.

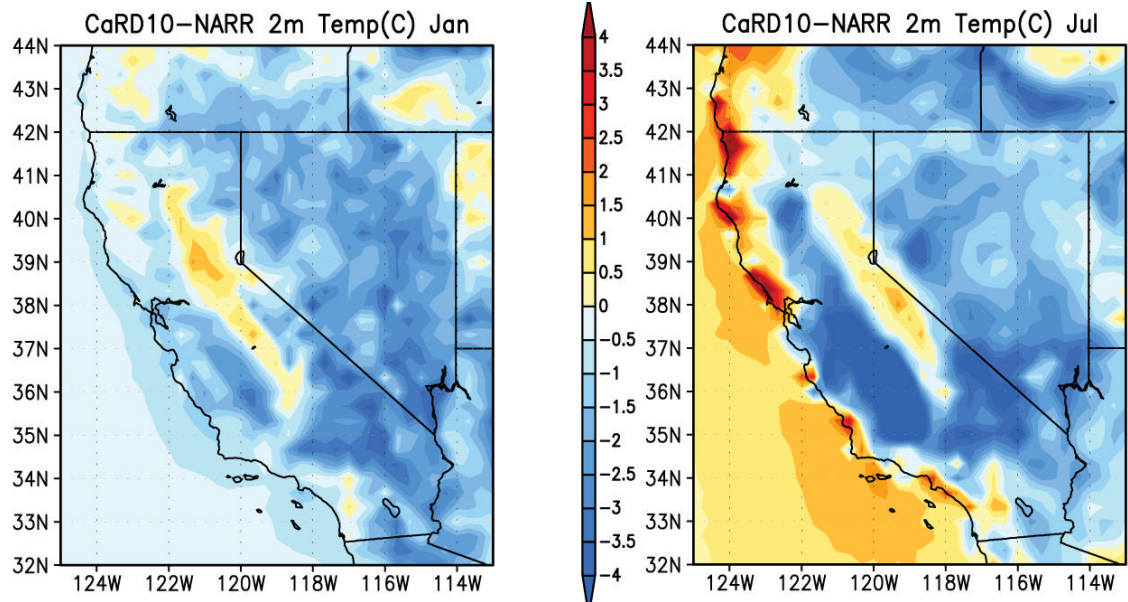


Figure 5 2 m temperature difference (K) between CaRD10 and NARR in January and July.

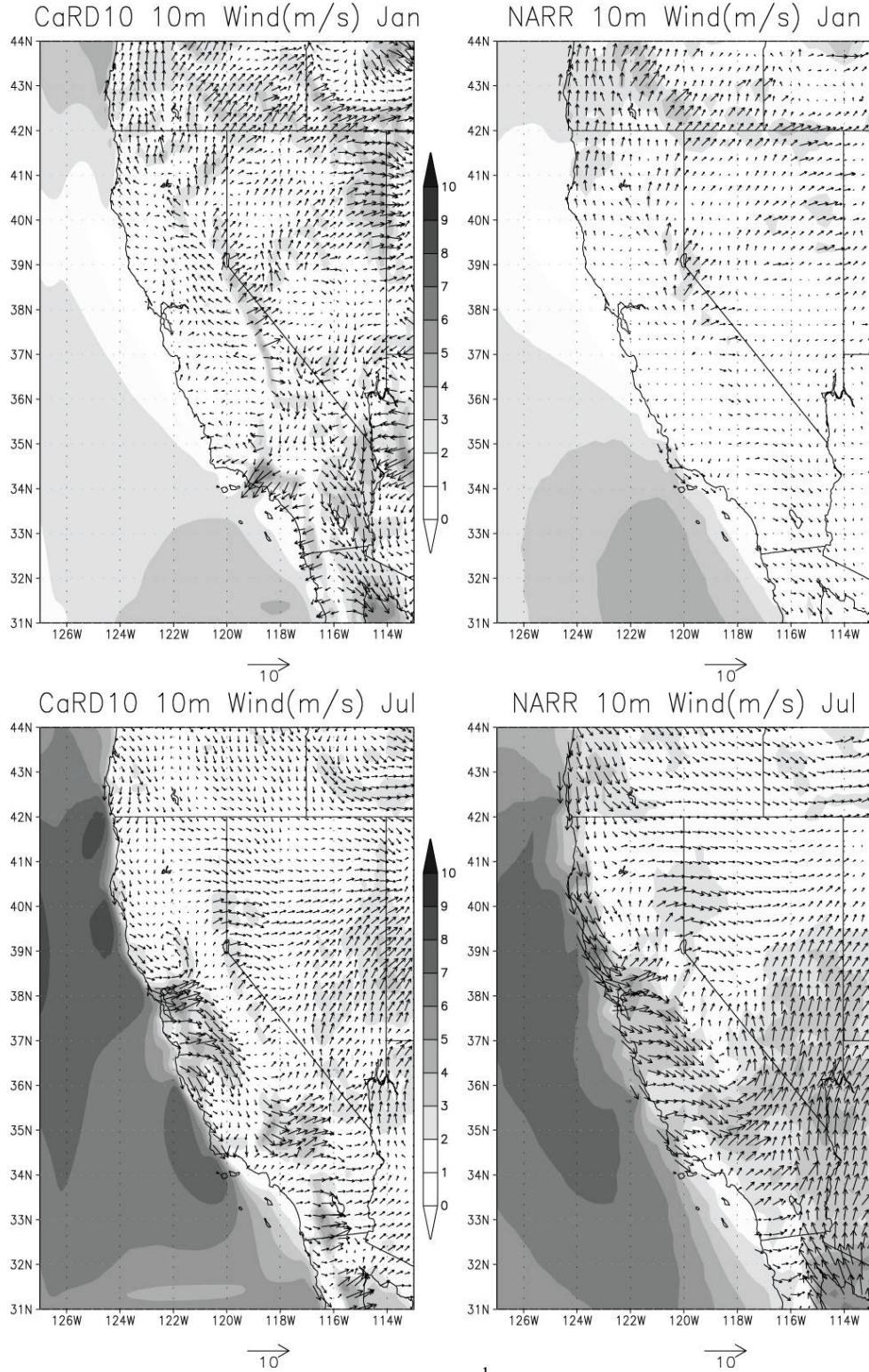


Figure 6 Comparison of 10 m wind (m s^{-1}) between CaRD10 (left) and NARR (right) in January (top panels) and July (bottom panels).

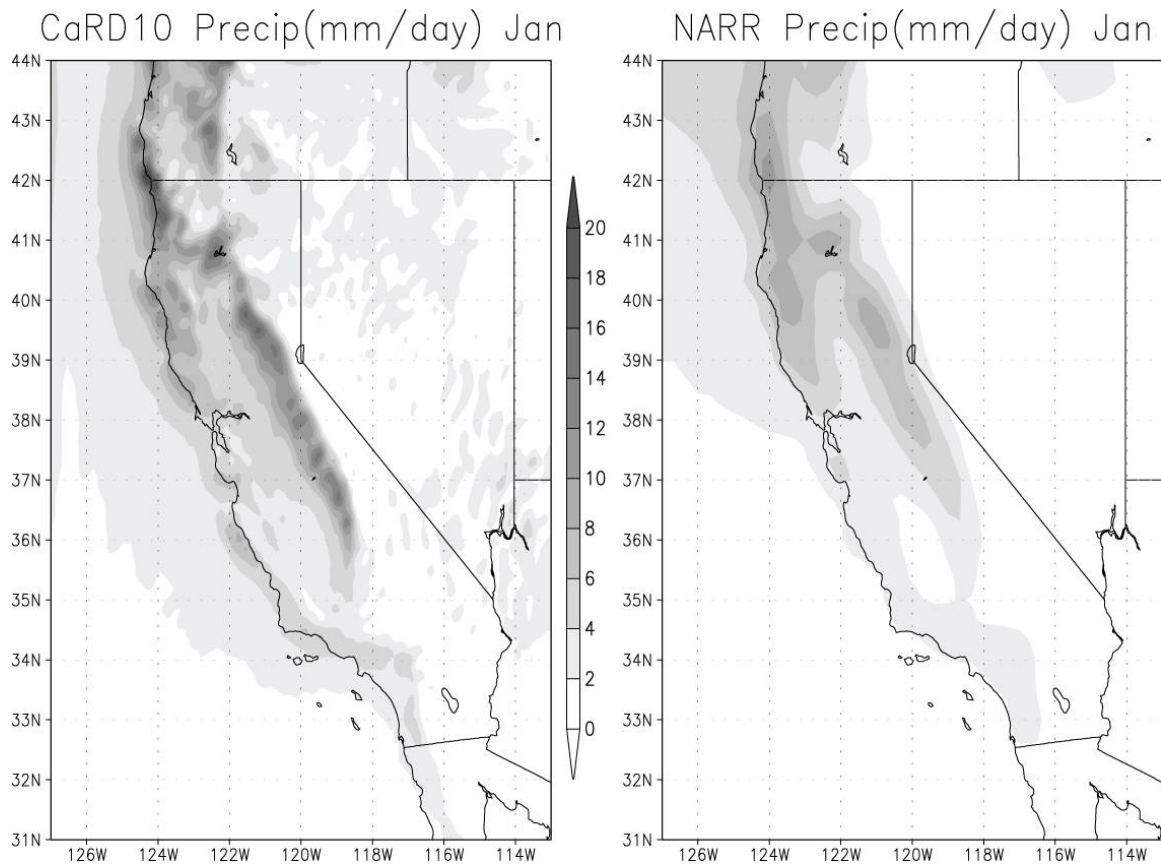


Figure 7 Comparison of January mean (1979-2002) precipitation rate (mm day^{-1}) between CaRD10 (left) and NARR (right).

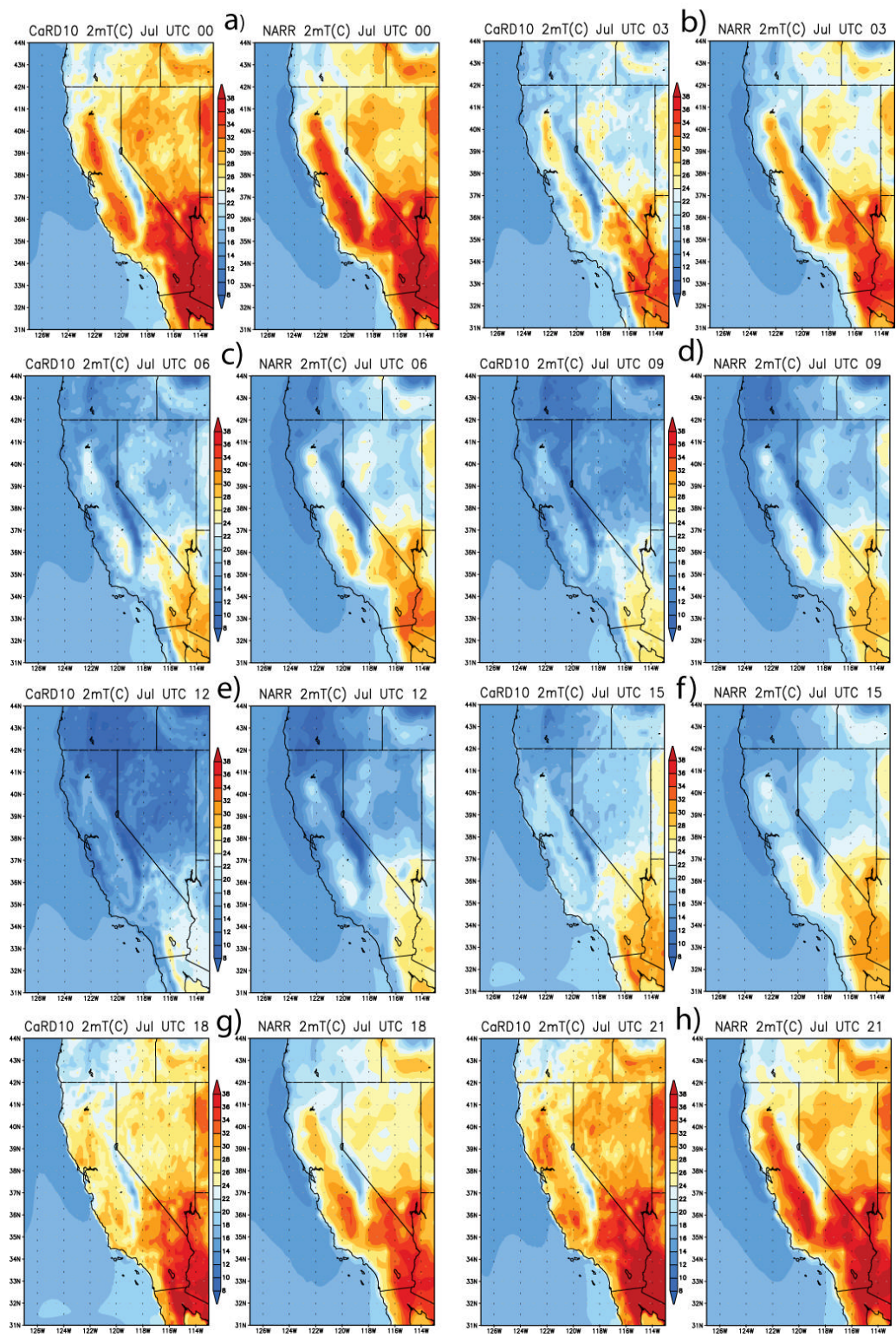
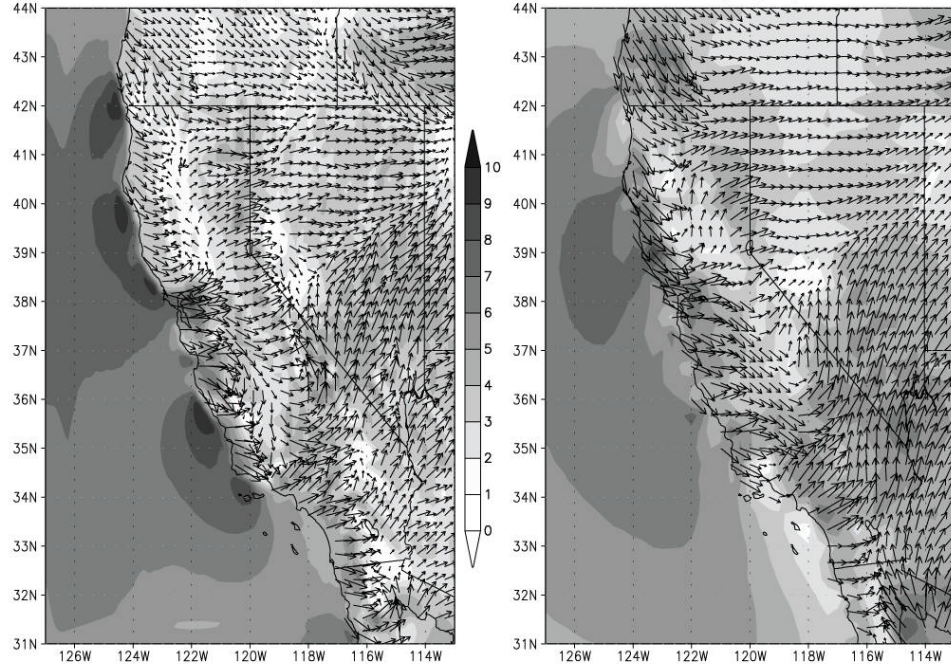


Figure 8 Comparison of diurnal variation of July 2 m temperature between CaRD10 (left) and NARR (right) at 3 hour intervals from 00 UTC to 21 UTC.

CaRD10 10mWin(m/s) Jul UTC 00 NARR 10mWin(m/s) Jul UTC 00



CaRD10 10mWin(m/s) Jul UTC 06 NARR 10mWin(m/s) Jul UTC 06

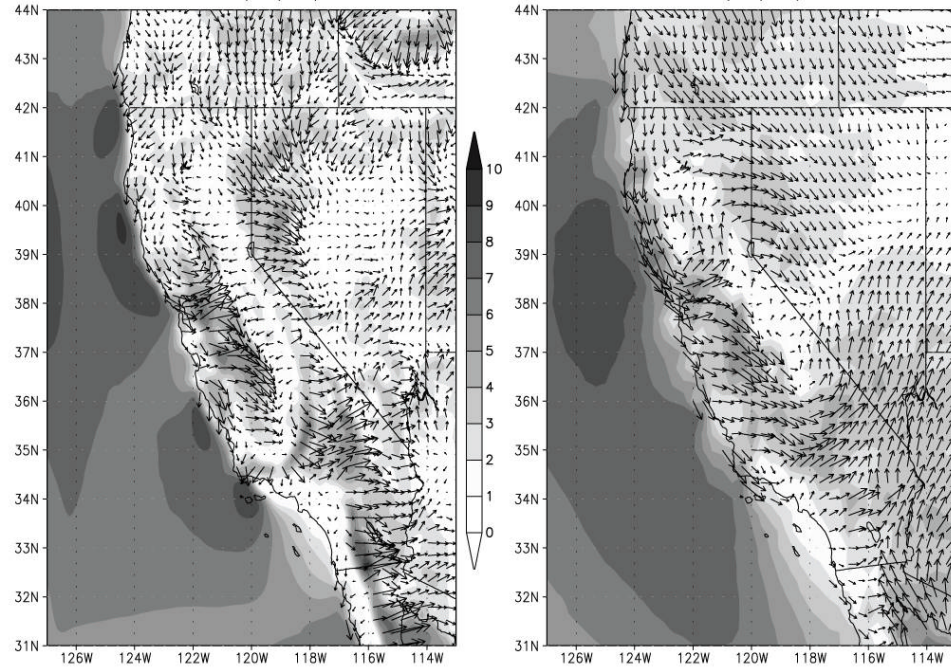


Figure 9 Comparison of July 10 m wind (m s^{-1}) between CaRD10 (left) and NARR (right) at 00 UTC (upper panels) and 06 UTC (lower panels).

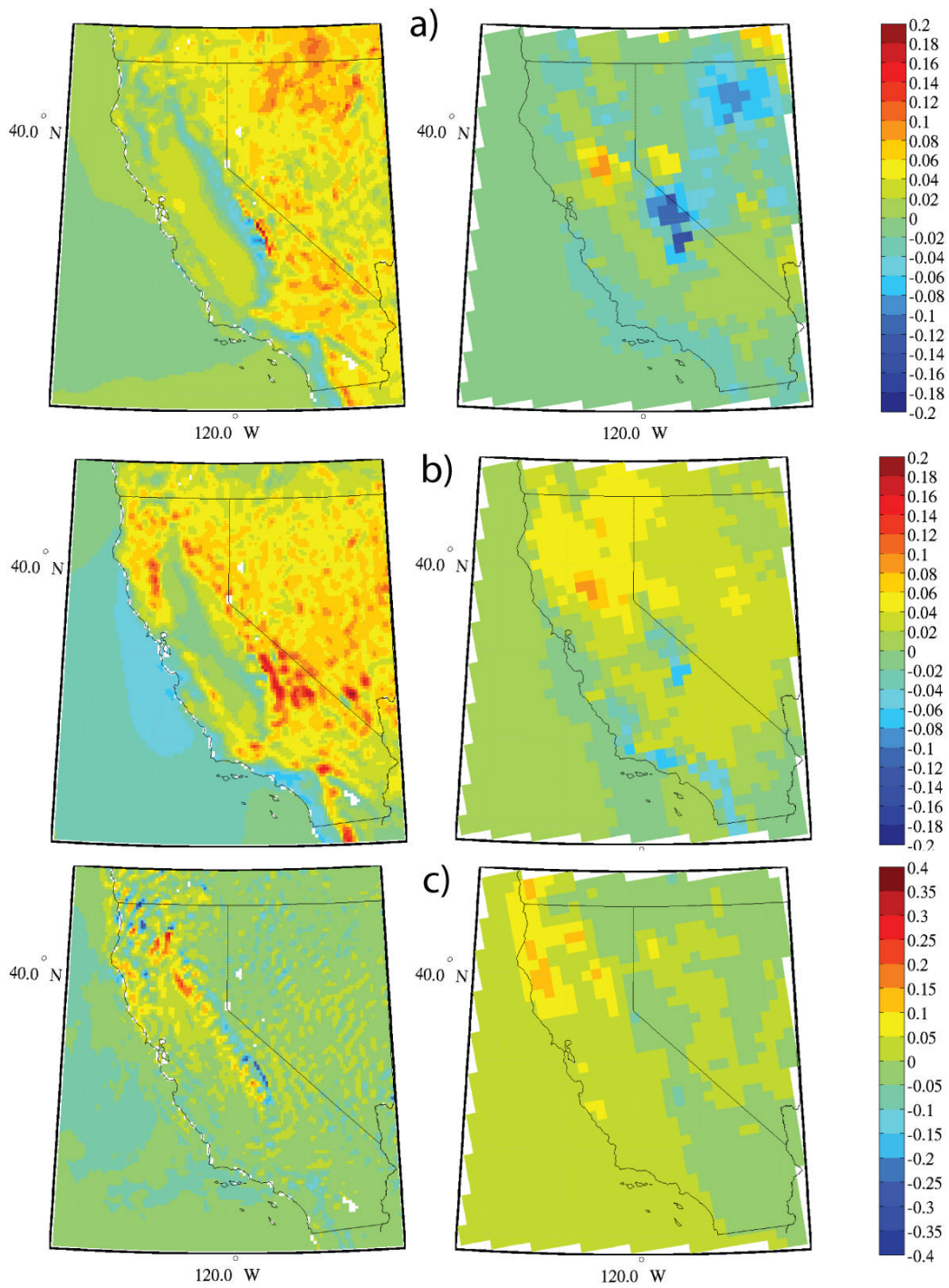


Figure 10 Comparison of trend for the period 1979 to 2002 between CaRD10 (left) and NARR (right). a) 2 m temperature trend (K year^{-1}) in DJF, b) 2 m temperature trend (K year^{-1}) in JJA, and c) precipitation rate trend ($\text{m day}^{-1} \text{ year}^{-1}$) in DJF.

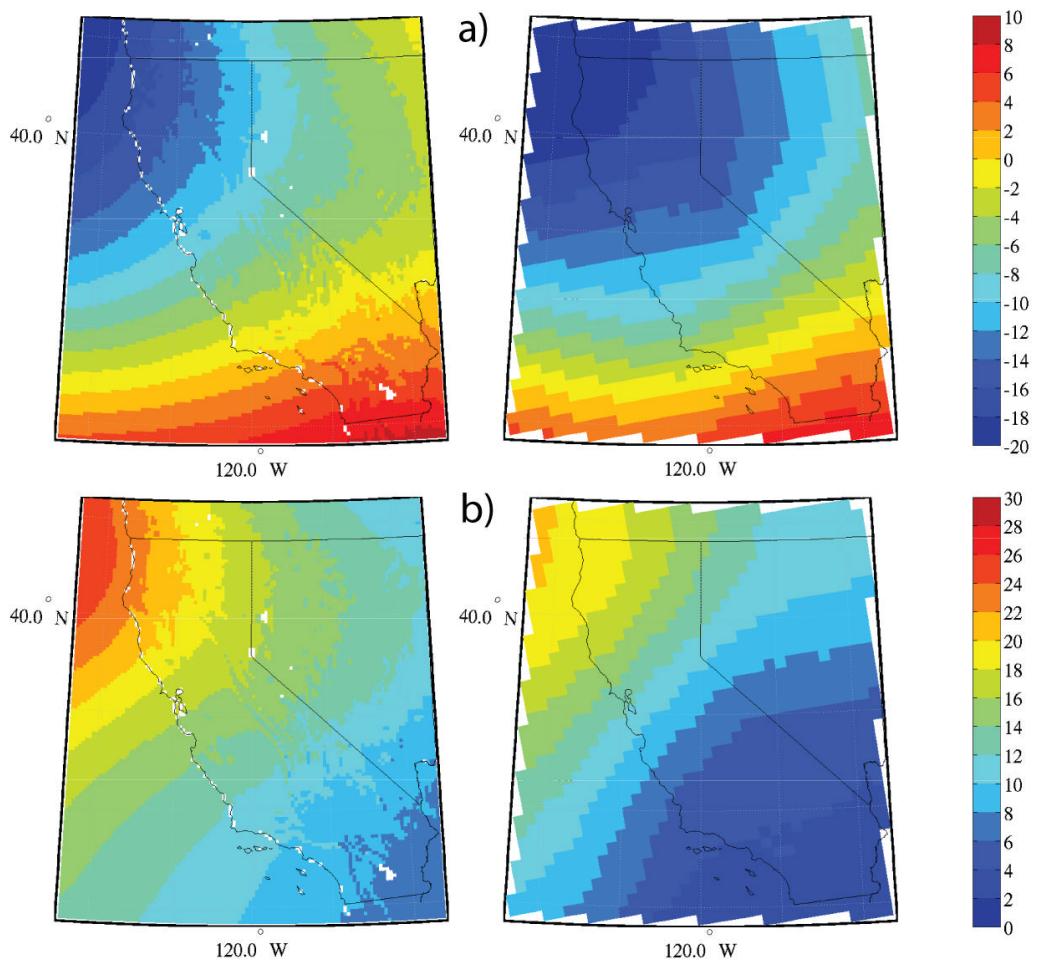
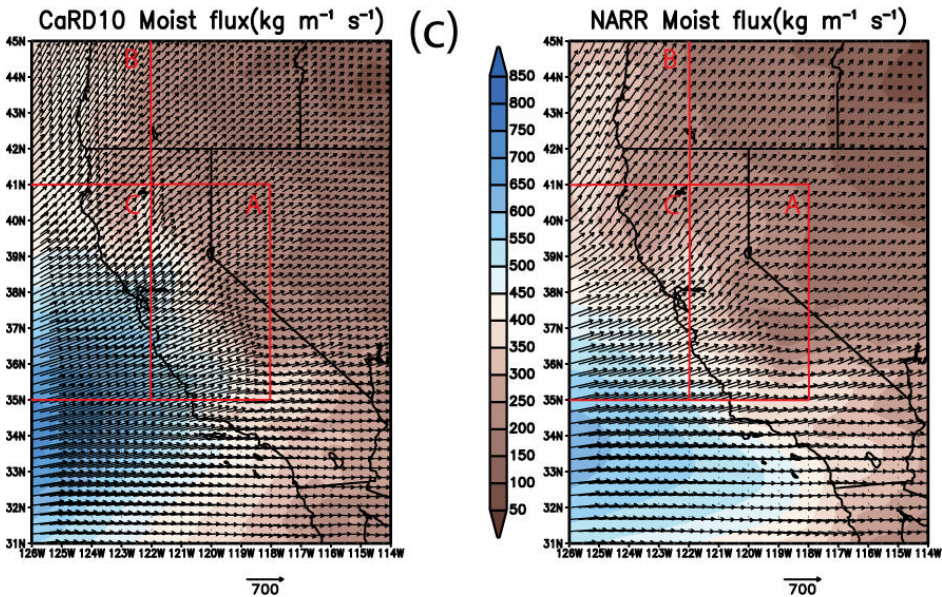
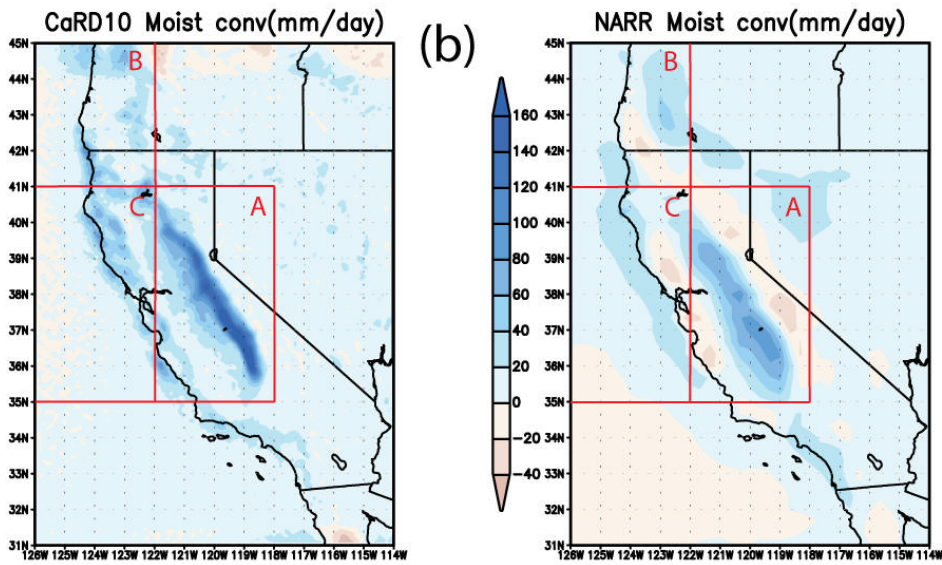
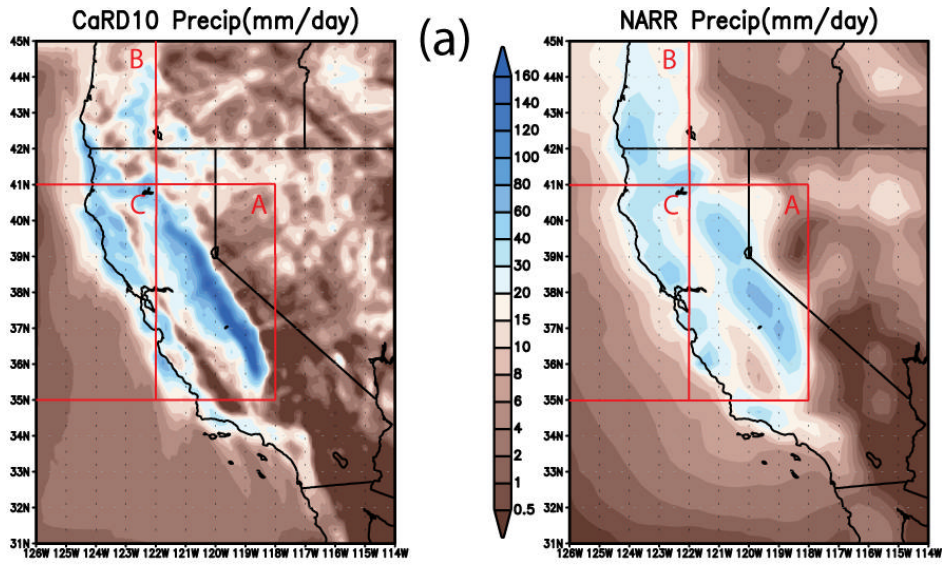


Figure 11 Comparison of 500-hPa height trend (m/23years) for the period 1979 to 2002 between CaRD10 (left) and NARR (right) in (a) DJF and (b) JJA.



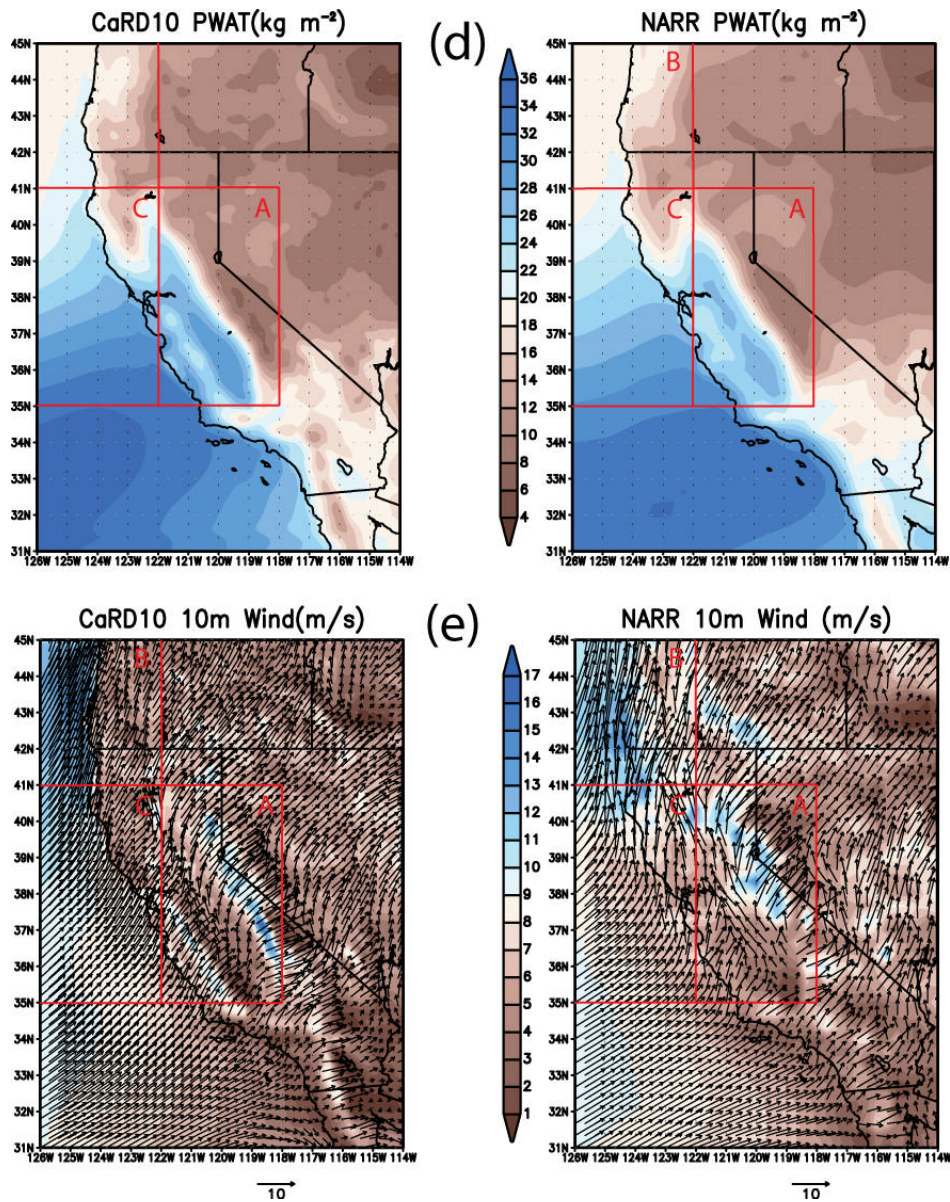


Figure 12 Comparison of a storm event on 7-9 November 2002. Left column is CaRD10 and right column is NARR. (a) Precipitation (mm day^{-1}) (b) Moisture convergence (mm day^{-1}) (c) Vertically integrated moisture flux ($\text{kg m}^{-1} \text{s}^{-1}$) (d) Precipitable water (kg m^{-2}), and (e) 10m wind (m s^{-1}). Superimposed are areas A to C for the water budget study.